

Three-Dimensional Nanographene Based on Triptycene: Synthesis and Its Application in Fluorescence Imaging

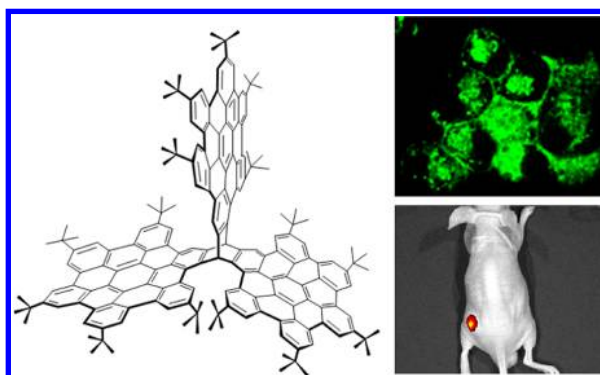
Chun Zhang,^{*,†} Ying Liu,[†] Xiao-Qin Xiong,[†] Lian-Hui Peng,[†] Lu Gan,^{*,†}
Chuan-Feng Chen,^{*,‡} and Hui-Bi Xu[†]

College of Life Science and Technology, Huazhong University of Science and Technology, and National Engineering Research Center for Nanomedicine, Hubei, 430074, China, and Beijing National Laboratory for Molecular Sciences, CAS Key Laboratory of Molecular Recognition and Function, Institute of Chemistry, Chinese Academy of Sciences, Beijing 100190, China

chunzhang@hust.edu.cn; lugan@hust.edu.cn; cchen@iccas.ac.cn

Received October 15, 2012

ABSTRACT



A novel kind of three-dimensional (3D) nanographene based on a triptycene structure bearing three hexa-*peri*-hexabenzocoronene (HBC) moieties was synthesized efficiently from triiodotriptycene. With the characteristic of intrinsic fluorescence, the 3D nanographene was used as a fluorescent agent for *in vitro* and *in vivo* fluorescence imaging with good antiphotobleaching ability and little toxicity.

Hexa-*peri*-hexabenzocoronene (HBC) and its derivatives, namely nanographenes,^{1,2} have recently attracted great interest because they are recognized as promising building blocks for organic nanoelectronic and photovoltaic devices with their large π -systems and strong assembly abilities. So far, various devices based on nanographene molecules with different structures and functionalities have been well developed by organic synthetic or supramolecular protocols,

such as Aida's nanotubes,³ Li's graphene quantum dots,⁴ and Müllen's graphene nanoribbons and large graphenes.^{2,5} These HBC-based building blocks are all planar structures. Although three-dimensional (3D) structures might afford nanographenes, with new opportunities to improve their properties to reduce the face-to-face interaction between π -planes and increase their solubility like other organic materials,⁶ no such molecules have hitherto been reported. Moreover, as a consequence of the difficulty of water

[†] Huazhong University of Science and Technology.

[‡] Beijing National Laboratory for Molecular Sciences.

(1) For recent reviews, see: (a) Feng, X.; Pisula, W.; Müllen, K. *Pure Appl. Chem.* **2009**, *81*, 2203. (b) Müllen, K.; Rabe, J. *Acc. Chem. Res.* **2008**, *41*, 511.

(2) For recent examples of nanographenes, see: (a) Cai, J.; Ruffieux, P.; Jaafar, R.; Bieri, M.; Braun, T.; Blankenburg, M.; Muoth, M.; Seitsonen, A. P.; Saleh, M.; Feng, X.; Müllen, K.; Fasel, R. *Nature* **2010**, *466*, 470. (b) Yang, S.; Feng, X.; Zhi, L.; Cao, Q.; Maier, J.; Müllen, K. *Adv. Mater.* **2010**, *22*, 838.

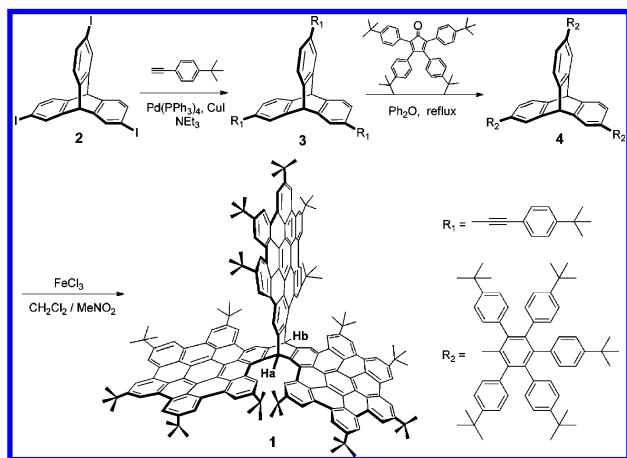
(3) (a) Zhang, W.; Jin, W.; Fukushima, T.; Saeki, A.; Seki, S.; Aida, T. *Science* **2011**, *334*, 340. (b) He, Y.; Yamamoto, Y.; Jin, W.; Fukushima, T.; Saeki, A.; Seki, S.; Ishii, N.; Aida, T. *Adv. Mater.* **2010**, *22*, 829. (c) Zhang, W.; Jin, W.; Fukushima, T.; Ishii, N.; Aida, T. *Angew. Chem., Int. Ed.* **2009**, *48*, 4747.

(4) (a) Yan, X.; Cui, X.; Li, B.; Li, L.-S. *J. Am. Chem. Soc.* **2010**, *132*, 5944. (b) Yan, X.; Cui, X.; Li, L.-S. *Nano Lett.* **2010**, *10*, 1869.

(5) Wu, J.; Pisula, W.; Müllen, K. *Chem. Rev.* **2007**, *107*, 718 and references therein.

solubilization, the biological applications of HBCs have remained largely unexplored, especially in fluorescence imaging.⁷ In this area, the problem of photobleaching for fluorescent agents has become a great obstacle. Although some antiphotobleaching fluorescent agents such as quantum dots have been successfully developed, the potential toxicity of heavy metals has greatly limited their biomedical applications. Searching for fluorescence imaging agents with high stability and little toxicity is still a challenge.⁸

Scheme 1. Synthesis of 3D Nanographene **1**



Triptycenes, with unique three-dimensional rigid frameworks, have more applications in materials science^{9,10} and molecular machines.¹¹ Recently, we¹² utilized the useful building blocks to construct novel hosts and subsequently develop a series of new supramolecular systems. Herein, we describe the synthesis of triptycene derived three-dimensional nanographene **1**, which bears three HBC moieties in the triptycene three-dimensional scaffold. With the characteristic of intrinsic fluorescence, the three-dimensional

nanographene aqueous nanoparticles can be prepared for fluorescence imaging with little cytotoxicity. Moreover, the 3D nanographene displayed good antiphotobleaching ability compared to other commercial fluorescent agents such as LysoTracker Green. These results encourage further studies of our 3D nanographene for biomedical applications like graphene.¹³

Synthesis of the 3D nanographenes is outlined in Scheme 1. Starting from triiodotriptycene **2**,¹⁴ its palladium-catalyzed Sonogashira coupling reaction with *tert*-butylphenylacetylene in the presence of Pd(PPh₃)₄, CuI, and NEt₃ afforded triethynylation product **3** in good yield, which was then subjected to a Diels–Alder reaction with *tert*-butylphenylcyclopentadienone¹⁵ to result in the polyphenylene dendritic precursor **4** in 43% yield. Oxidative cyclization of **4** with FeCl₃/MeNO₂ in CH₂Cl₂ resulted in the formation of 3D nanographene **1** as a pale yellow solid in 87% yield.

In the ¹H NMR spectrum of **1**, two sharp singlet signals appeared at δ 8.26 and 8.91 ppm for the two methenyl protons (Ha and Hb) of the triptycene scaffold, which were assigned by 2D C–H COSY analysis (Figure S7). The formation of 3D nanographenes was furthermore confirmed by the MALDI-TOF mass spectrum.¹⁶ As shown in Figure S8, the mass spectrum of **1** revealed a peak at *m/z* 2429 for M⁺. Comparison of the MALDI-TOF spectrum of the 3D nanographene with that of its precursor **4** (Figure S9) indicated the elimination of 36 hydrogen atoms during the Scholl oxidative condensation reactions occurred, which is consistent with the differences between the molecular formulas of 3D nanographene (C₁₈₈H₁₇₀) and its precursor **4** (C₁₈₈H₂₀₆). The infrared vibrational spectra showed more simple absorption peaks in this range of the aromatic C–H out-of-plane bending vibration (650–950 cm⁻¹) of **1** compared with **4**, which afforded further evidence of the formation of 3D nanographene (Figure S10).^{4b} The absorption and emission spectra of the 3D nanographene were obtained in dichloromethane solution. When **1** was excited at 364 nm ($\epsilon = 3.05 \times 10^5 \text{ M}^{-1} \text{ cm}^{-1}$, 298 K), the emission wavelength at 470, 490, and 500 nm with a fluorescent quantum yield of 12.8% was observed (Figures S11 and S12).

To direct the biological application of our 3D nanographene, water solubilization is necessary. Adding the THF solution of **1** to a water containing poly(ethylene glycol)-*block*-poly(propylene glycol)-*block*-poly(ethylene glycol) (pluronic F68) nonionic surfactant could prepare the aqueous nanoparticles of **1** after removing THF by rotary evaporation (Figure 1a).¹⁷ For the aqueous nanoparticles

(6) (a) Mori, S.; Nagata, M.; Nakahata, Y.; Yasuta, K.; Goto, R.; Kimura, M.; Taya, M. *J. Am. Chem. Soc.* **2010**, *132*, 4054. (b) Long, T. M.; Swager, T. M. *Adv. Mater.* **2001**, *13*, 601.

(7) Yin, M.; Shen, J.; Pisula, W.; Liang, M.; Zhi, L.; Müllen, K. *J. Am. Chem. Soc.* **2009**, *131*, 14618.

(8) Some recent examples of 2D nanographene/nanographene oxide for fluorescence imaging with antiphotobleaching property: (a) Li, J.-L.; Bao, H.-C.; Hou, X.-L.; Sun, L.; Wang, X.-G.; Gu, M. *Angew. Chem., Int. Ed.* **2012**, *52*, 1830. (b) Pan, D.; Guo, L.; Zhang, J.; Xi, C.; Xue, Q.; Huang, H.; Li, J.; Zhang, Z.; Yu, W.; Chen, Z.; Li, Z.; Wu, M. *J. Mater. Chem.* **2012**, *22*, 3314.

(9) For recent reviews, see: (a) Swager, T. M. *Acc. Chem. Res.* **2008**, *41*, 1181. (b) Chong, J. H.; MacLachlan, M. J. *Chem. Soc. Rev.* **2009**, *38*, 3301 and references therein.

(10) For recent examples, see: (a) Zhang, C.; Liu, Y.; Li, B.; Tan, B.; Chen, C.-F.; Xu, H.-B.; Yang, X.-L. *ACS Macro. Lett.* **2012**, *1*, 190. (b) VanVeller, B.; Robinson, D.; Swager, T. M. *Angew. Chem., Int. Ed.* **2012**, *51*, 1182. (c) Mastalerz, M.; Schneider, M. W.; Oppel, I. M.; Presly, O. *Angew. Chem., Int. Ed.* **2011**, *50*, 1046.

(11) Kelly, T. R.; Cai, X.; Damkaci, F.; Panicker, S. B.; Tu, B.; Bushell, S. M.; Cornella, I.; Piggott, M. J.; Salives, R.; Caverio, M.; Zhao, Y.; Jasmijn, S. J. *Am. Chem. Soc.* **2007**, *129*, 376.

(12) (a) Zhu, X.-Z.; Chen, C.-F. *J. Am. Chem. Soc.* **2005**, *127*, 13158. (b) Zong, Q.-S.; Zhang, C.; Chen, C.-F. *Org. Lett.* **2006**, *8*, 1859. (c) Zhang, C.; Chen, C.-F. *J. Org. Chem.* **2007**, *72*, 3880. (d) Zhang, C.; Chen, C.-F. *J. Org. Chem.* **2007**, *72*, 9339. (e) Zhang, C.; Chen, C.-F. *CrystEngComm* **2010**, *12*, 3255. (f) Chen, C.-F. *Chem. Commun.* **2011**, *47*, 1674.

(13) (a) Robison, J. T.; Tabakman, S. M.; Liang, Y.; Wang, H.; Casalongue, H. S.; Vinh, D.; Dai, H. J. *J. Am. Chem. Soc.* **2011**, *133*, 6825. (b) Liu, Z.; Robinson, J. T.; Sun, X.; Dai, H. J. *J. Am. Chem. Soc.* **2008**, *130*, 10876.

(14) Zhang, C.; Chen, C.-F. *J. Org. Chem.* **2006**, *71*, 6626.

(15) Draper, S. M.; Gregg, D. J.; Madathil, R. *J. Am. Chem. Soc.* **2002**, *124*, 3486.

(16) Tomovic, Z.; Watson, M. D.; Müllen, K. *Angew. Chem., Int. Ed.* **2004**, *43*, 755.

(17) (a) Xiao, J.; Yin, Z.; Li, H.; Zhang, Q.; Boey, F.; Zhang, H.; Zhang, Q. *J. Am. Chem. Soc.* **2010**, *132*, 6926. (b) Liu, Q.; Yang, T.; Feng, W.; Li, F. *J. Am. Chem. Soc.* **2012**, *134*, 5390.

with a concentration of $5 \mu\text{g/mL}$, dynamic light scattering analysis displayed that the hydrodynamic size of these nanoparticles was maintained at 100 nm as shown in Figure 1b. The UV spectrum of the nanoparticles displayed the maximal absorption peak at 364 nm, which is similar to their dichloromethane solution. Excitation of the nanoparticles ($5 \mu\text{g/mL}$) in water at 364 nm resulted in a fluorescence emission at 475 and 504 nm with a shoulder at 557 nm (Figure 1c). Figure 1d shows a typical transmission electron micrograph (TEM) image of 3D nanographene nanoparticles with a size distribution of 40–50 nm.

With the characteristic of intrinsic fluorescence, the aqueous nanoparticles of 3D nanographene could be used as a fluorescent agent for cellular imaging with green fluorescence, as well as red fluorescence for human hepatocellular carcinoma HepG2 cells after 6 h of incubation with a concentration of $5 \mu\text{g/mL}$ (Figure S13). To further determine the cellular uptake process, the cellular imaging experiments were performed for human ovarian cell line A2780 and mouse leukemic monocyte macrophage cell line RAW264.7 using an Andor Revolution spinning disk confocal microscope when the cells were treated with aqueous nanoparticles ($5 \mu\text{g/mL}$) for multiple time points (i.e., 1, 3, and 6 h). As shown in Figure 2a, 3D nanographene nanoparticles can be readily detected in both A2780 and RAW264.7 cells after 1 h of incubation. As time went on, the fluorescence intensity increased and more nanoparticles were internalized into the cells. To examine the potential for *in vivo* imaging, subcutaneous injection of 3D nanographene **1** ($20 \mu\text{L}$ aliquots, 0.1 mg/mL) into the left flank of a nude mouse was administered. The signals were clearly observed when the mouse was imaged in a fluorescence mode (green fluorescent protein (GFP) excitation filter, 445–490 nm and dsRed emission filter, 570–650 nm) without any skin autofluorescence (Figure 2b). We next examined the biodistribution of 3D nanographene **1** after intravenous injection ($100 \mu\text{L}$ aliquots, 0.1 mg/mL). The results showed that 3D nanographene **1** mainly accumulated in the liver (Figure 2c).

For fluorescence imaging agents, the shortcoming of photobleaching greatly limits their biomedical application. To examine the intracellular photostability of 3D nanographene **1**, HepG2 cells were incubated with either the commonly used LysoTracker Green or 3D nanographene **1** for 1 h and were imaged over time during continuous excitation under a confocal microscope. At the zero time point, the fluorescence intensities of LysoTracker Green and 3D nanographene **1** were similar. After approximately 6 min of irradiation, the LysoTracker Green signal was almost completely photobleached, while the signal of 3D nanographene **1** was still readily detected (Figures 3 and S14). Furthermore, the cytotoxicity of 3D nanographene **1** was evaluated by the 3-(4, 5-dimethyl-2-thiazolyl)-2, 5-diphenyltetrazolium bromide (MTT) assay in A2780 and RAW264.7 cells. As shown in Figure S15, 3D nanographene **1** induced time- and concentration-dependent cytotoxicity; it only induced a less than 10% reduction in cell viability for A2780 and RAW264.7 cells, even at a concentration of $20 \mu\text{g/mL}$ for 6 h.

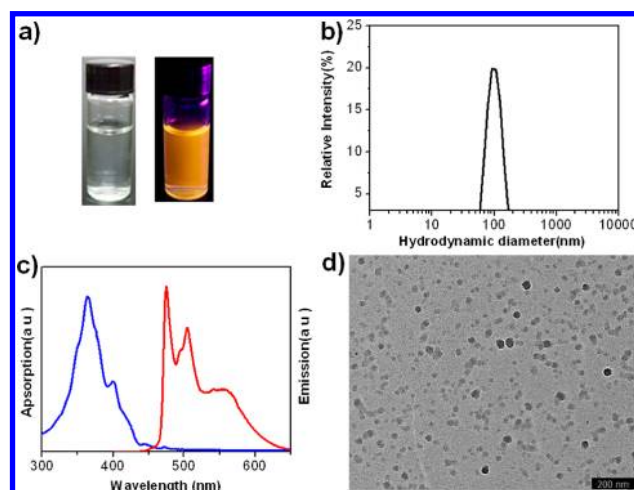


Figure 1. (a) Photographs under daylight (left) and under UV light (right), (b) hydrodynamic size with concentration of $5 \mu\text{g/mL}$, (c) UV (blue line) and fluorescent (red line) spectra, and (d) TEM image of 3D nanographene nanoparticles.

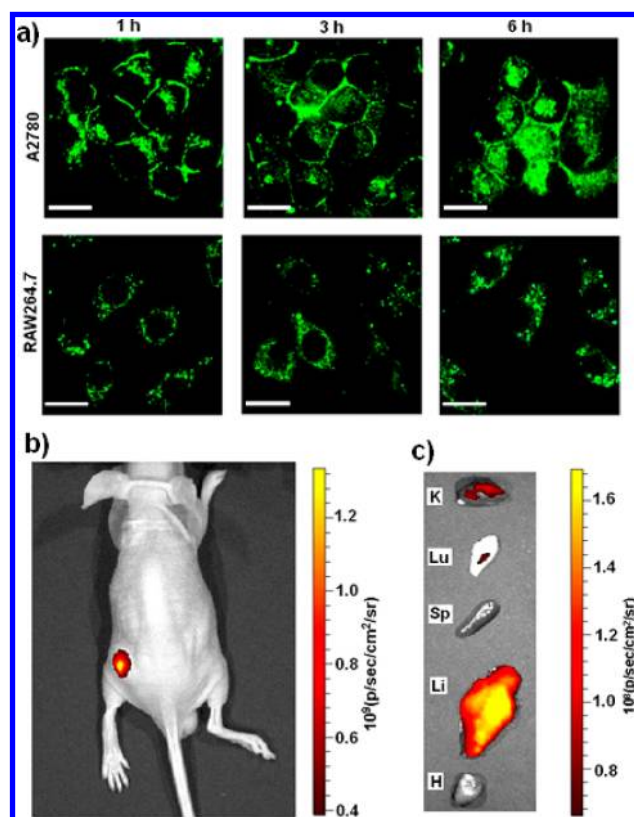


Figure 2. (a) *In vitro* cellular imaging with 3D nanographene nanoparticles in A2780 and RAW264.7 cells after 1 h, 3 and 6 h incubation. Scale bar: $50 \mu\text{m}$. (b) *In vivo* fluorescence image of 3D nanographene nanoparticles ($20 \mu\text{L}$ of 0.1 mg/mL) injected subcutaneously on the left flank of a mouse. (c) Fluorescence images showing the biodistribution of 3D nanographene nanoparticles in a mouse 1 h after injection. K, Lu, Sp, Li and H indicate kidney, lung, spleen, liver and heart, respectively.

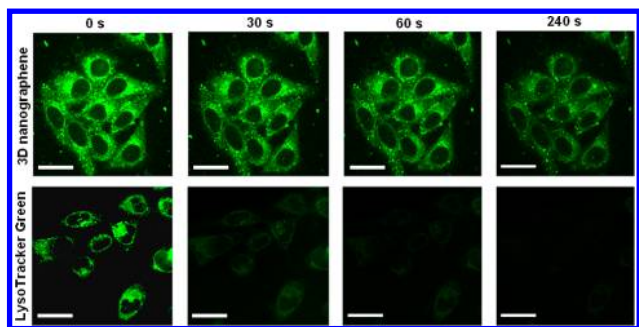


Figure 3. *In vitro* photostability after incubation with either LysoTracker Green or 3D nanographene nanoparticles in HepG2 cells. Scale bar: 50 μm .

In conclusion, we have synthesized a novel 3D nanographene **1** based on a triptycene scaffold and characterized its structure by NMR, MALDI-TOF MS, UV, fluorescence, and IR spectra. With its intrinsic fluorescence, 3D nanographene **1** can be employed for *in vitro* and *in vivo* fluorescence imaging, upon functionalization by a

nonionic surfactant to provide water dispersal and low toxicity. Much can be done in the future to load some anticancer drugs in the expanded “internal molecular free volume” of triptycene which can be used as a multifunctional theranostic platform for cancer treatment.

Acknowledgment. This work was supported by the National Natural Science Foundation of China (20902031), the National Basic Research Program (2012CB932500, 2011CB933103, and 2011CB932501), the Fundamental Research Funds for the Central Universities (HUST 2011TS148), and Wuhan ChenGuang Program (201150431118). We also thank the Analytical and Testing Center of Huazhong University of Science and Technology for related analysis.

Supporting Information Available. Details of experimental materials and measurements, synthetic procedures for **1**, FT-IR and UV spectra of **1** and **4**, Fluorescent emission spectra of **1**, *in vitro* and *in vivo* fluorescence imaging, photostability and MTT experiments. This material is available free of charge via the Internet at <http://pubs.acs.org>.

The authors declare no competing financial interest.